An integrated scheme based on stacked denoising autoencoder and deep feature fusion for fault diagnosis of helicopter planetary gear train

Canfei Sun
College of Automation Engineering
Nanjing University of Aeronautics and Astronautics
Aviation Key Laboratory of Science and Technology on Fault Diagnosis and Health Management
Nanjing, China
suncanfei@samri.com.cn

Youren Wang
College of Automation Engineering
Nanjing University of Aeronautics and Astronautics
Nanjing, China
wangyrac@nuaa.edu.cn

Liang Cao
Research Center
Shanghai Aero Measurement & Control Technology Research Institute
Shanghai, China
hdcaoliang@163.com

***Abstract*—Planetary gear train plays a critical role in the helicopter transmission system. Fault diagnosis of the planetary gear train has long been a research topic in the health monitoring and maintenance of the helicopter. However, due to the intricate kinematics and severe operating conditions, the vibration signals of the planetary gear train are highly complex, dominated by various coupling disturbances and ambient noise. Aiming to address these challenges, an integrated health state identification scheme (IHSIS) is proposed for fault diagnosis of helicopter planetary gear train. Firstly, IHSIS utilizes multiple sensors to collecting vibration signals for sufficient fault information under multi-mode faults and fluctuating working conditions. Secondly, stacked denoising automatic encoder (SDAE) is adopted to explore deep features from frequency spectrum of each individual sensor. Finally, deep features derived from measured signals of all sensors are fused together and input to a softmax classifier for fault diagnosis. The superiority of IHSIS is validated by analyzing results of a few comparative experiments conducted on a helicopter main-rotor testbed with intentionally created localized gear faults of a planetary gear train under different noise levels.**

Keywords-Helicopter; Planetary gear train; Fault diagnosis; Stacked denoising autoencoder; Feature fusion.

I. INTRODUCTION

Planetary gear trains are widely used in helicopter transmission systems on various rotorcrafts for their distinctive characteristic of large reduction ratio, high bearing capacity and tight configuration. Once the planetary gear train fails, it may lead to transmission deficiency, even shutdown of the entire helicopter transmission system. Therefore, fault diagnosis and health management of planetary gear train is very important and necessary to ensure helicopter flight safety [1-2].

To date, numbers of techniques have applied in fault diagnosis of planetary gearboxes, but most of these contributions were not completely verified for helicopter applications [3-7]. Compared to common planetary gearboxes, vibration signals measured from the helicopter planetary gear train are more special and complex with a variety of synchronization vibration components and heavy background noise. All these effects would weaken the low-frequency vibration signatures of faulty components concealed in measured vibration signals, and substantially increase the degree of difficulty in fault diagnosis of the helicopter planetary gear train. Therefore, the effectiveness of those fault diagnosis techniques developed for common planetary gearboxes would be reduced or even disappeared when applied to helicopter planetary gear trains.

For addressing the issue, researchers have explored various types of diagnostic methods based on models, signal processing, and pattern recognition for fault diagnosis of helicopter planetary gear train [8-10]. The studies have significantly enriched the literature in this field. However, most researches only focused on single sensor vibration signals analysis. On account of complex and diversified behaviors, the vibration signals collected by a single sensor sometimes cannot extract the most sensitive feature information on the fault, consequently the weak fault characteristics and limited information would affect diagnosis accuracy. Because multisensor measured signals always possess the redundant and complementary information, and can produce the reliable and high-quality representation for diagnosis, some researches have put forward a variety of multisensor information fusion methods to diagnose rotating machinery [11-13].

As a breakthrough in machine learning, in recent years, deep learning has been vigorously developed and widely used in artificial intelligence and other fields [14-15]. By imitating the mechanism of human brain, deep learning-based methods

978-1-7281-0860-5/19/$31.00 ©2019 IEEE

attempt to excavate high-level representations from low-level input through deep neural network architecture. Two typical and powerful deep learning networks, stacked autoencoder (SAE) and deep belief network (DBN), have been successfully applied to data fusion, feature extraction and categories identification in fault diagnosis. Tamilselvan and Wang [16] implemented the health diagnosis of aircraft engines and power transformers through the application of DBN, and achieved high precision compared with the existing diagnostic technology. Chen et al. [17] succeeded in employing DBN directly to diagnose gearbox fault with the raw vibration signals. Tan et al. [18] proposed an intelligent method based on SAE and wavelet transform to achieve roller bearing fault diagnosis. Liu et al. [19] employed SAE to realize gearbox fault diagnosis through extracting effective feature representation from frequency-domain signals. As can be seen that most methods above based on SAE or DBN have successfully applied to explore salient features or classify mechanical failures. However, for fault diagnosis of the helicopter planetary gear train, the adaptability of these algorithms is still worth discussing under the strong influence of the severe environmental noise and fluctuating load.

Recently, as an extension of SAE, stacked denoising autoencoder (SDAE) has been presented to learn robust feature representation using a deep network architecture with a local denoising criterion [20]. Some researchers developed diagnostic methods based on SDAE and achieved satisfying results in rotating machine fault diagnosis. Lu et al. [21] proposed a detailed and empirical study of SDAE under different noise levels and fluctuating loads for fault diagnosis of rotary machinery components. Xia et al. [22] applied a deep neural network (DNN) based on SDAE for fault diagnosis of a bearing unit, and successfully achieved correct classification under newly occurring conditions. Thirukovalluru et al. [23] utilized SDAE to obtain good feature representations from handcrafted features and good classification performance for bearing fault diagnosis. Jiang et al. [24] presented a multilevel SADE based feature representation learning approach for fault diagnosis of wind turbine gearbox test rig, and obtained satisfactory diagnosis accuracy. These studies demonstrated SDAE is particularly suitable for fault identification with respect to complex signals containing ambient noise in the real operating environment.

In this paper, we proposed an integrated health state identification scheme (IHSIS) for the helicopter planetary gear train fault diagnosis. Firstly, multiple sensors are utilized to acquire vibration signals, so that redundant and complementary information can be achieved. Secondly, SDAE is conducted to extract fault features from frequency spectrum, and finally these features derived from all sensors are fused and input to a softmax classifier to identify fault modes.

The remainder of the paper is organized as follows. A brief introduction of the preliminaries of this paper is provided in Section II. In Section III, the general procedure of IHSIS is described. Section IV introduces the experimental setting and validates the effectiveness and robustness of IHSIS by analyzing the experiment results. Conclusion is presented in Section V.

II. PRELIMINARIES

A. Denoising autoencoder

As a symmetrical three-layer neural network, autoencoder (AE) is architected by coding network and decoding network. Target to realizing a feature reconstruction, the outputs are requested to be similar to the inputs as possible through unsupervised learning mechanism that applies backpropagation. A situation always happens in the practical environment that the samples are easily corrupted by the ambient noise, creating great trouble in the learning process. Base on this issue, a new denoising mechanism is brought in AE network, known as denoising autoencoder (DAE), to realize the robust feature representations extraction for the noisy samples. In DAE structure displayed in Figure1, the encoding network introduces "noise" with special statistical properties to the input samples, which still employed as the goal of reconstruction for the model. Hence, DAE aims to capture the statistical architecture in the original samples and obtain better feature representations by minimizing reconstruction difference in the unsupervised learning process. The DAE model applied in this paper is illustrated as follows.

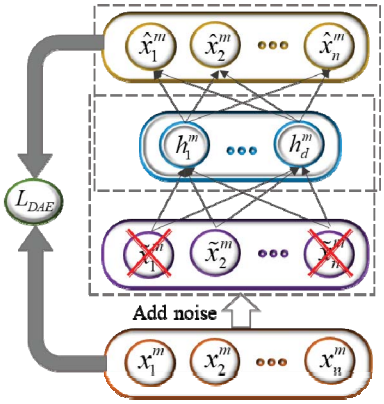

Figure 1. Structure of denoising autoencoder.

Let q_D be a random noise distribution, the corruption part is represented by a stochastic mapping:

$$\tilde{\boldsymbol{x}}^m \sim q_D(\tilde{\boldsymbol{x}}^m \mid \boldsymbol{x}^m) \tag{1}$$

where $\boldsymbol{x}^m$ and $\tilde{\boldsymbol{x}}^m$ are the original samples and corrupted samples, $m = 1,2...,M$, and M is the sample size. Hereafter, the corrupted samples $\tilde{\boldsymbol{x}}^m$ is mapped to $\boldsymbol{h}^m$ in the hidden layer:

$$\begin{cases} \boldsymbol{h}^m = f_\theta(\boldsymbol{W}\tilde{\boldsymbol{x}}^m + \boldsymbol{b}) = \text{sigmoid}\,(\boldsymbol{W}\tilde{\boldsymbol{x}}^m + \boldsymbol{b}) \\ \theta = \{\boldsymbol{W}, \boldsymbol{b}\} \end{cases} \tag{2}$$

where $\boldsymbol{W}$ and $\boldsymbol{b}$ denote the weight and bias parameters in the encoding process, respectively.

The following decoding network reconstructs $\boldsymbol{x}^m$ through remapped $\boldsymbol{h}^m$ to $\hat{\boldsymbol{x}}^m$ in the output layer:

$$\begin{cases} \hat{\boldsymbol{x}}^m = f_{\theta'}(\boldsymbol{W}'\boldsymbol{h}^m + \boldsymbol{b}') \\ \theta' = \{\boldsymbol{W}', \boldsymbol{b}'\} \end{cases} \tag{3}$$

where $\boldsymbol{W}'$ and $\boldsymbol{b}'$ stand for the weight and the bias parameters in the decoding process.

The reconstruction error function L_{DAE} between $\hat{\boldsymbol{x}}^m$ and $\boldsymbol{x}^m$ to be minimized during the training process is indicated:

$$L_{DAE} = \arg\min_{\boldsymbol{W},\boldsymbol{W}',\boldsymbol{b},\boldsymbol{b}'} \frac{1}{M} \sum_{m=1}^{M} \left\| \hat{\boldsymbol{x}}^m - \boldsymbol{x}^m \right\|^2 \tag{4}$$

After training with the corrupted samples, DAE model is robust in the case of the contaminated signal or samples deficiencies.

B. SDAE

The SDAE employs a stacked network architecture comprised of a series of cascading DAEs, as shown in Figure 2. In general, for representing better high-order feature representations, the number of neurons need to be gradually decreasing layer by layer, and the greedy layer-wise unsupervised learning is applied to DAE model level by level. The pre-training and fine-tuning process is included in the model construction of SDAE.

In pre-training process, the training sample $\boldsymbol{x}^m$ is used to train DAE1 and encoded as:

$$\boldsymbol{h}_1^m = f_{\theta_1}(\boldsymbol{W}_1\boldsymbol{x}^m + \boldsymbol{b}_1) \tag{5}$$

where θ_1 is the parameter set of DAE1. As a hidden representation for $\boldsymbol{x}^m$, $\boldsymbol{h}_1^m$ is inputted into subsequent DAE, then DAE2 is similarly initialized and mapped $\boldsymbol{h}_1^m$ to $\boldsymbol{h}_2^m$. Repeats the same conversion until the last DAEn is trained and $\boldsymbol{h}_N^m$ is obtained.

$$\boldsymbol{h}_N^m = f_{\theta_N}(\boldsymbol{W}_N\boldsymbol{h}_{N-1}^m + \boldsymbol{b}_N) \tag{6}$$

After pre-training initializes each successive DAE to implement layered feature representations extraction and transmit the hidden regularity throughout the cascading construction, the whole SDAE model enters a supervised training process to fine-tune network parameters.

In fine-tuning, $\boldsymbol{h}_N^m$ is transmitted to a supervised classifier, and the parameters derived from pre-training are determined by the global back propagation optimization process.

The output z^m is defined as:

$$\boldsymbol{z}^m = g_{\theta_{N+1}}(\boldsymbol{h}_N^m) \tag{7}$$

where $\boldsymbol{\theta}_{N+1}$ denotes network parameters of the output layer, and $g(\cdot)$ stand for the softmax classifier in this study employed for multi-class classification. We suppose the label $\boldsymbol{y}^m$ is the training target, corresponding to the training sample $\boldsymbol{x}^m$,for supervised optimization learning. Thereafter, SDAE performs fine tuning by minimizing the cross entropy loss function L_{SDAE}.

$$L_{SDAE} = \arg\min_{\Theta} \frac{1}{M} \sum_{m=1}^{M} [\boldsymbol{y}^m \ln \boldsymbol{z}^m - (1-\boldsymbol{y}^m)\ln(1-\boldsymbol{z}^m)] \tag{8}$$

where $\boldsymbol{\Theta}$ is SDAE model parameters and $\boldsymbol{\Theta} = \{\boldsymbol{\theta}_1, \boldsymbol{\theta}_2, \cdots, \boldsymbol{\theta}_{N+1}\}$.

After unsupervised learning process in pre-training and supervised learning process in fine-tuning, the SDAE model is established and a high-order feature representation of the training samples is achieved.

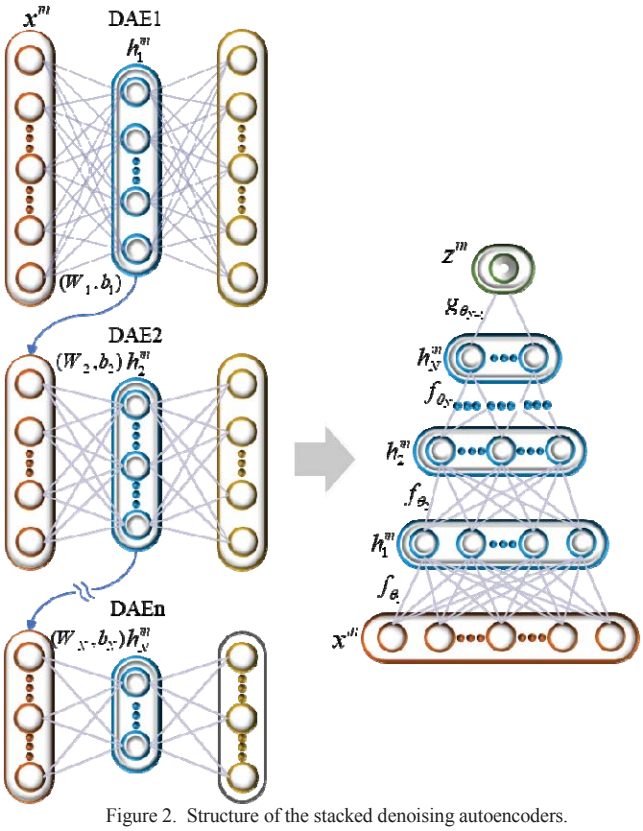

Figure 2. Structure of the stacked denoising autoencoders.

III. IHSIS

The flowchart of IHSIS is shown in Figure 3, and the detailed description of each step is summarized as follows.

(1) Multi-sensor signals acquisition.

Step1. Determine the number of sensor M and measurement point through layout analysis.

Step2. Synchronous acquisition of vibration signals through a signal acquisition device under all candidate failure modes respectively.

(2) IHSIS model construction.

Step1. Calculate the frequency spectrum of the raw signals of each sensor and divided them into training samples and testing samples.

Step2. Given training samples and fault labels, number of hidden layers, number of neurons for each layer, noise factor, for establishment of an optimal SDAE model.

Step3. Pre-train and Fine-tune the SDAE with all training samples, finally obtain the optimized parameters set.

Step4. Repeat the previous step to complete SDAEs training for all sensors, and determine all deep features for subsequent fusion diagnosis.

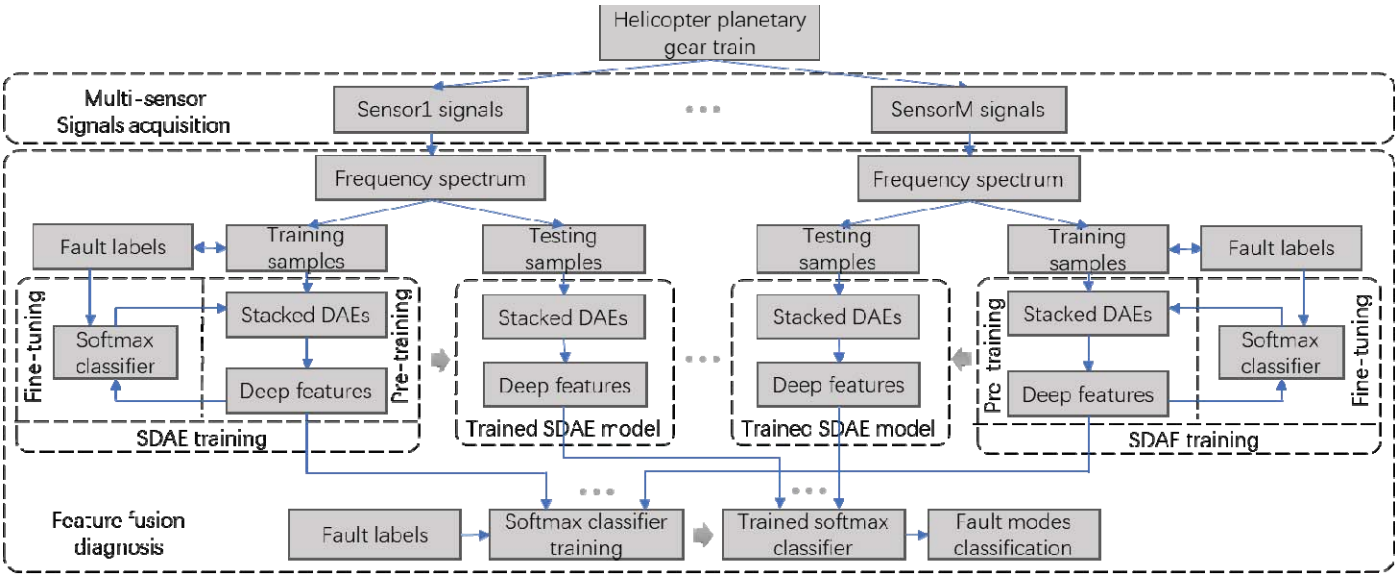

Figure 3. Schematic diagram of IHSIS.

Step5. Given training samples, fault labels and trained SDAEs, complete softmax classifier training based on fused features.

(3) Feature fusion diagnosis

Step1. Given testing samples and trained IHSIS, including trained SDAEs and softmax classifier, for fault modes classification.

Step2. Complete health state identification of all samples, and generate classification accuracy.

IV. EXPERIMENTS

A. Experimental Setup

In this study, a helicopter main rotor testbench displayed in Figure 4 is introduced to generate the experimental dataset. The testbench consists of a high-power motor, a compound gearbox contained a planetary gear train, a variable load and several signal acquisition devices. Two kinds of localized fault, the cracked and spalling tooth, are introduced to the sun and one planet gear respectively. Therefore, including normal and four gear fault modes, there is a total of five fault categories, denoted as C0 to C4. The vibration signals are collected synchronously by three accelerometers adhered to the main rotor housing with a sampling rate of 20kHz. To reduce the computational burden, all the measured signals are resampled at a sampling frequency of 5kHz to cover the minimum effective frequency band (0-2.5kHz). Each sample measured by each sensor has 2500 data points. The dataset of each fault category is divided into 800 training samples and 200 test samples, and a total of 5,000 samples are collected for the five fault categories.

Because of having an impact on classification accuracy, main structural parameters of all deep learning models in IHSIS and the comparative algorithms are determined through experimental analysis as described as follows: firstly, a certain number of samples are randomly selected from the test dataset, then continuously adjusts the values of these parameters through evaluating the classification accuracy, which is defined as the ratio of correct classification numbers to total categories. finally, the parameter values corresponding to the highest classification accuracy in all tested samples are taken as the final decision.

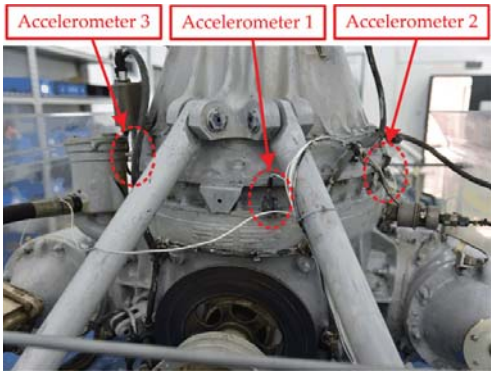

Figure 4. Helicopter transmission test rig used for the experiment.

B. Experimental Results

To demonstrate the superiority of IHSIS, five other methods are introduced to compare with IHSIS. The first and second, denoted as IHSIS1 and IHSIS2, replace SDAE with SAE and DBN as fault modes classification algorithm and other processing are the same as in IHSIS. The third is support vector machine (SVM), which is a traditional classification model that widely used to fault diagnosis based on a group of common features of gearboxes. The last two algorithms are SAE and DBN, which directly identify health state with the raw data. To illustrate the strengths of multi-sensor feature fusion, the

samples of each single sensor is also tested by six methods independently with the same conditions. Table I displays the comparison results.

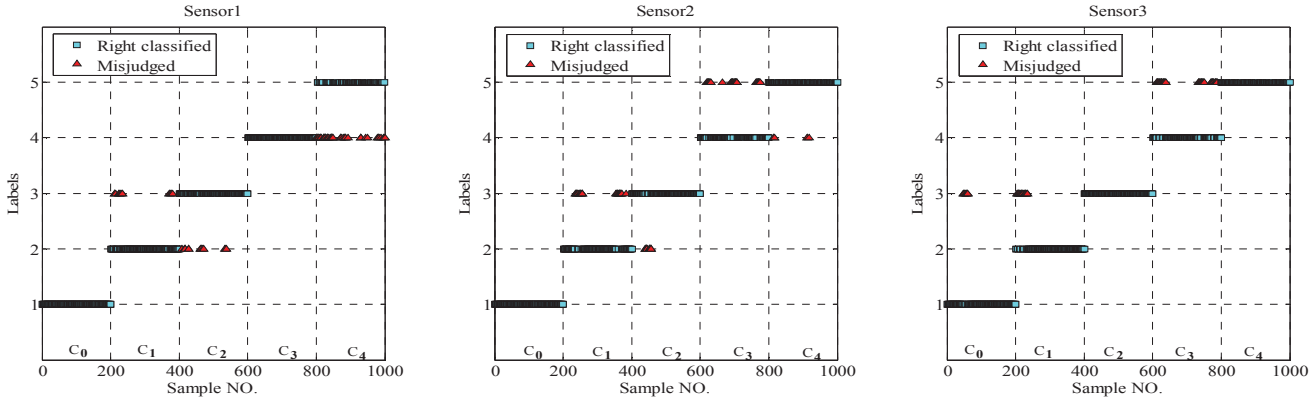

Figure 5. The classification results of three individual sensors.

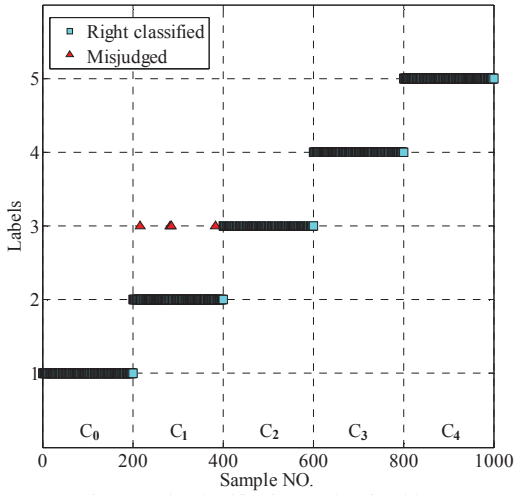

Figure 6. The classification results of multi-sensor.

happens to the comparative methods too, and the values are 5.63%, 5.28%, 5.21%, 3.95%, and 4.24%, respectively, for the IHSIS1, IHSIS2, SVM, SAE, and DBN. Therefore, six methods all achieve obviously higher accuracy of multi-sensor fusion than that of any individual sensor. This shows that multi-sensor captures more valuable information about gear fault than any single sensor, and the fusion diagnosis of these information effectively improves the accuracy of classification.

TABLE I. COMPARISON RESULTS OF CLASSIFICATION ACCURACY.

Algorithms	**Classification Accuracy**			
	Sensor1	***Sensor2***	***Sensor3***	***Multi-sensor***
IHSIS	93.75%	92.54%	93.22%	99.63%
IHSIS1	92.86%	88.65%	90.74%	96.38%
IHSIS2	91.37%	89.62%	92.83%	96.55%
SVM	88.25%	87.34%	86.68%	92.63%
SDAE	90.24%	91.36%	89.65%	94.37%
DBN	89.92%	90.63%	88.27%	93.85%

From the classification results, IHSIS exhibits high correct classification rates in multi-sensor, which higher 6.46% than the average results of three single sensor. This situation

By observation, SVM achieves worst results compared with other tested algorithms based on deep learning. Moreover, IHSIS, IHSIS1 and IHSIS2 perform better than SAE and DBN, which employ raw measured data as input vector directly. In addition, compared to IHSIS1 and IHSIS2, IHSIS produces a higher result no matter in multisensor or single sensor. For example, IHSIS has a highest classification accuracy of about 93.75% in three single sensors, and nearly 0.89% larger than that of IHSIS1 (92.86%), and 0.92% for IHSIS2 (92.83%). Moreover, the difference reaches close to 3.25% and 3.08%, respectively, in multi-sensor, indicating that IHSIS has significant potential for health state identification of helicopter planetary gear train.

In order to further illustrate the identification effect of IHSIS more intuitive, a group of detailed classification result under different fault modes are given in Figure 5 and 6. The method based on each single sensor is represented as sensors 1, 2, or 3, corresponding to the three individual sensors.

As can be seen from the classification results of three individual sensors in Figure 5, each sensor gains excellent per-formance in certain fault modes identification. For example, sensor 1 correctly identify all the samples in C0 and C3, and the same situation happens with sensor2 for C0, and sensor3 for C2 and C4. However, they do not perform as well in other certain modes, and numbers of samples are misjudged into wrong fault classes, such as sensor1 for C4, sensor2 for C1 and C3, and sensor3 for C3. Compared with single sensor, multisensor performs significantly better as the detailed demonstration in Figure 6, only individual samples are misclassified from C1 into C2. The reasonable explanation is as follows. For each measurement, the most desirable effect is that the meshing vibration signal of the faulty gear is transmitted to the sensor in the shortest and simplest path. For example, if one sensor is installed in the position of each ring gear tooth, the local failure meshing vibration of any gear tooth of any planetary gear can be measured by the sensor in the most direct way. It is impossible to arrange so many sensors under realistic conditions. However, compared to a single fixed-point mounted sensor, sensors installed in multiple different

locations increase the probability of this most effective measurement because faulty gear meshing vibrations can be measured with a shorter transfer path by one of the closest sensors. Therefore, in the case of multiple failure modes, the multisensor measured signal contains more intense and richer fault-sensitive information and achieves more desirable results.

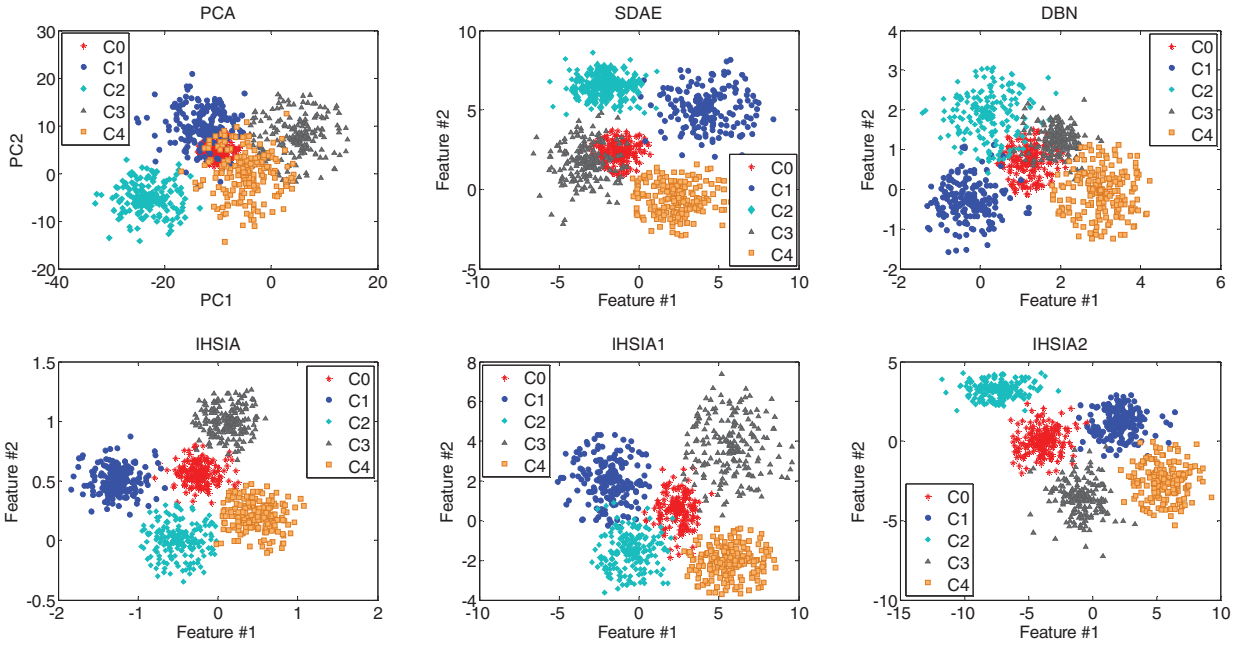

Figure 7. The clustering results of two-dimensional features extracted by the comparative methods.

In general, a group of high-level feature representation is essential to achieve high classification accuracy. To further evaluate the features explored by the employed algorithms, a comparative experiment is carried out. All algorithms based on deep learning are conducted to reconstruct the input data to two-dimensional features, and all input features for SVM is reduced dimension to two principal features by the principal component analysis (PCA). The discrimination ability of these two-dimensional features is demonstrated intuitively by a clustering analysis, as displayed in Figure 7.

From the results, seriously overlaps are observed in PCA, and apart from C2, other models are basically difficult to distinguish. The same situation also happens in SDAE and DBN between C0 and C3, and the clusters are difficult to separate from each other. In IHSIS1 and IHSIS2, some overlaps are existed between C0 and other modes. Compared with the above algorithms, IHSIS performs relatively better, only slight overlaps happen between C0 and C3, and obvious separations are observed in other modes, indicating that IHSIS exhibits the excellent ability of learning high-level feature representations with high robustness.

C. *Noise Environment Testing*

In the operation of the helicopter, the working environment is constantly changing, which directly influences the measured vibration signal. The electromagnetic disturbance caused by the variation of external electromagnetic environment can easily contaminate the vibration signals through conduction or radiation, forming severe background noise and reducing the signal to noise ratio (SNR). Therefore, we design an experiment to validate the performance of fault diagnosis method under the variational background noise.

In this experiment, noise environment testing is executed to validate the effectiveness and robustness of IHSIS with different SNR values. By adopting cross validation method, all samples of each fault category are randomly divided into training data and testing data by the ratio of 4:1, and the testing samples are synthesized with the ambient noise with different SNRs. The average classification accuracy of five times stand-alone run is served as the final result, as shown in Table II.

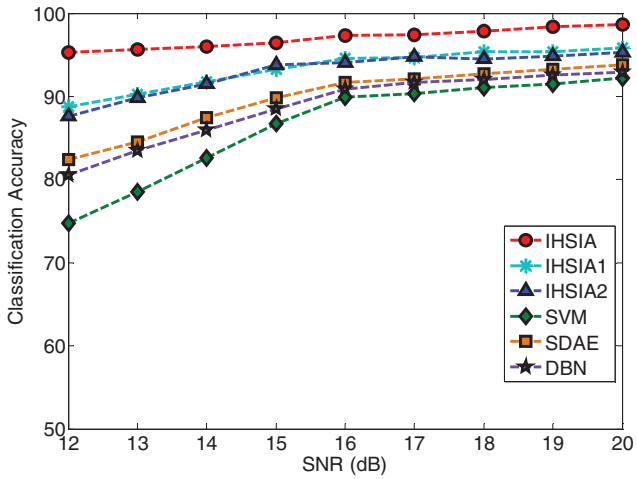

Figure 8. Classification results of six methods with different SNRs.

From the average results, basically all the methods achieve good classification accuracy above 91% when the SNR is higher than 18dB. For example, the values are 98.63%, 95.78%, 95.25%, 92.22%, 93.78% and 92.90%, respectively, for the IHSIS, IHSIS1, IHSIS2, SVM, SDAE and DBN methods at 20dB. However, a clear downward trend followed with the decline of SNR, as shown in Figure 8. Compared with SVM for shallow learning, the other methods based on deep learning models exhibit better classification accuracy for most of SNRs, owing to a deeper unsupervised learning network structure and a stronger learning capability

TABLE II. COMPARISON RESULTS OF CLASSIFICATION ACCURACY.

Algorithms	Classification Accuracy								
	12dB	13dB	14dB	15dB	16dB	17dB	18dB	19dB	20dB
IHSIS	95.25%	95.66%	96.02%	96.42%	97.35%	97.37%	97.83%	98.35%	98.63%
IHSIS1	88.72%	90.23%	91.75%	93.28%	94.56%	94.63%	95.35%	95.37%	95.78%
IHSIS2	87.58%	89.83%	91.46%	93.78%	94.03%	94.79%	94.46%	94.83%	95.25%
SVM	74.73%	78.49%	82.54%	86.73%	89.86%	90.32%	91.04%	91.49%	92.22%
SDAE	82.38%	84.53%	87.46%	89.78%	91.63%	92.09%	92.75%	93.23%	93.78%
DBN	80.53%	83.49%	85.94%	88.53%	90.86%	91.68%	92.04%	92.56%	92.90%

for the complex nonlinear mapping between input data and fault categories. Besides, compared to SDAE and DBN based on raw data, IHSIS, IHSIS1 and IHSIS2 have higher correct classification rates, especially when SNRs are less than 16dB. As an example, IHSIS1 gets an accuracy improvement of 8.19% than DBN in the 12dB. Furthermore, as indicated by the classification results, IHSIS performs relatively accurately to IHSIS1 and IHSIS2, showing an increased accuracy of 6.53% and 7.67% respectively at 12dB, for example. It illustrates that SDAE-based health state identification in IHSIS exerts its advantages through encodes and reconstructs by adding noise, which effectively reduces the effect of noise on insufficient fault information and improves the robustness of data representation.

Through the above-mentioned study, IHSIS synthesizes both merits of multi-sensor complementary fault information fusion and anti-noise in SDAE-based feature extraction, which offers outstanding classification results under low SNRs. Therefore, it demonstrates that IHSIS is superior in the field of the health state identification for helicopter planetary gear train under the working conditions with strong ambient noise.

V. CONCLUSIONS

(1) The harsh working conditions, such as strong background noise and fluctuating loads, coupled with the unique structure, make it difficult to obtain satisfactory results for the fault diagnosis of helicopter planetary gear train. To address this issue, an integrated health state identification algorithm denoted as IHSIS is developed in this paper, congregated the virtues of multisensor signal acquisition, SDAE-based feature extraction and fusion diagnosis.

(2) SDAE-based deep learning model exhibits the strong learning ability of feature representations and high noise robustness, and the fusion of these high-quality deep features maximally exploits the complementary information derived from each individual sensor, which further guarantees the applicability of IHSIS under strong background noise and load fluctuation.

(3) The comparative experiments are conducted between IHSIS and the other algorithms employed in gear fault diagnosis, and the experimental results demonstrate the effectiveness and robustness of IHSIS for fault diagnosis of helicopter planetary gear train under the sever working conditions.

Acknowledgements

This research is supported by the Aeronautical Science Foundation of China (No. 2013ZD52055) and the Fundamental Research Funds for the Central Universities & Funding of Jiangsu Innovation Program for Graduate Education under Grant (No. KYLX16_0336).

References

1. D. M. Blunt and J. A. Keller, “Detection of a fatigue crack in a uh-60a planet gear carrier using vibration analysis,” *Mech. Syst. Signal Process*., vol. 20, no. 8, pp. 2095-2111, 2006.
2. C. F. Sun and Y. Y. Wang, “Advance in study of fault diagnosis of helicopter planetary gears,” *Chin. J. Aeronaut.*, vol. 38, no. 7, pp.106-119, 2017.(in chinese)
3. M. Zhao, M. Kang, B. Tang, and M. Pecht, “Deep residual networks with dynamically weighted wavelet coefficients for fault diagnosis of planetary gearboxes,” *IEEE Trans. Ind. Electron.,* vol. 65, no. 5, pp. 4290-4300, 2018.
4. Y. Qin, J. Zou, and F. Cao, “Adaptively detecting the transient feature of faulty wind turbine planetary gearboxes by the improved kurtosis and iterative thresholding algorithm,” *IEEE Access*, vol. 99, pp. 1-11, Mar. 2018.
5. Y. Li, Y. Yang, G. Li, M. Xu, and W. Huang, “A fault diagnosis scheme for planetary gearboxes using modified multi-scale symbolic dynamic entropy and MRMR feature selection,” *Mech. Syst. Signal Process*., vol. 91, pp: 295-312, 2017.
6. K. Feng, K. Wang, Q. Ni, M. J. Zuo, and D. Wei, “A phase angle based diagnostic scheme to planetary gear faults diagnostics under non-stationary operational conditions,” *J. Sound Vib.*, vol. 408, pp. 190-209, 2017.
7. J. Parra and C. M. Vicuña, “Two methods for modeling vibrations of planetary gearboxes including faults: comparison and validation,” *Mech. Syst. Signal Process.* vol.92, pp. 213-225, 2017.

8. F. Lei, S. Wang, X. Wang, H. Feng, and L. Huawei, “Nonlinear dynamic modeling of a helicopter planetary gear train for carrier plate crack fault diagnosis, ” *Chin. J. Aeronaut.,* vol. 29, no. 3, pp.675-687, 2016.

2004 IEEE Systems Readiness Technology Conference (AUTOTESTCON 2004), San Antonio, TX, USA, 20-23 September 2004; vol.61, pp.475-481.

11. Y. Lin, Y. Li, X. Yin, and Z. Dou, “Multi-sensor fault diagnosis modeling based on the evidence theory,” IEEE Trans. Rel., vol. 99, pp.1-9,2018.
12. L. Jing, T. Wang, M. Zhao, and P. Wang, “An adaptive multi-sensor data fusion method based on deep convolutional neural networks for fault diagnosis of planetary gearbox,” *Sensors*, vol. 17, no. 2, pp. 414-429, 2017.
13. Z. Chen, and W. Li, “Multi-sensor feature fusion for bearing fault diagnosis using sparse autoencoder and deep belief network,” *IEEE Tran. Instrum. Meas.*,vol. 66, no. 7, pp. 1693-1702, 2017.
14. G. E. Hinton, and R. R. Salakhutdinov, “Reducing the dimensionality of data with neural networks,” *Science*, vol. 313, pp. 504–507, 2006.
15. B. Schölkopf, J. Platt, and T. Hofmann, “Greedy layer-wise training of deep networks,” Advances in Neural Information Processing Systems 19: Proceedings of the 2006 Conference, vol. 19, pp. 153-160, 2007.
16. P. Tamilselvan, P. Wang, “Failure diagnosis using deep belief learning based health state classification,” *Reliab. Eng. Syst. Saf.*, vol. 115, pp. 124–135, 2013.
17. Z. Chen, C. Li, and R. V. Sánchez, “Multi-layer neural network with deep belief network for gearbox fault diagnosis,” *J. Vibroeng.*,vol. 17, pp. 2379–2392, 2015.
18. T. Junbo, L. Weining,; A. Juneng, and W. Xueqian, “Fault diagnosis method study in roller bearing based on wavelet transform and
9. N. Sawalhi, “Vibration sideband modulations and harmonics separation of a planetary helicopter gearbox with two different configurations,” *Adv. Acoust. Vib.*, vol. 2016, no. 1, pp. 1-9, 2016.
10. B. Wu, A. Saxena, T. S. Khawaja, and R. Patrick, “An approach to fault diagnosis of helicopter planetary gears,” In Proceedings of the

stacked auto-encoder,” In Proceedings of the 27th Chinese Control and Decision Conference (2015 CCDC), Qingdao, China, 23–25 May 2015; pp. 4608–4613.

19. L. Guifang, B. Huaiqian , and H. Baokun, “A Stacked Autoencoder-Based Deep Neural Network for Achieving Gearbox Fault Diagnosis,” *Math. Probl. Eng.*, vol. 2018, pp. 1-10, 2018.
20. P. Vincent, H. Larochelle, I. Lajoie, Y. Bingio, and P. A. Manzagol, “Stacked Denoising Autoencoders: Learning Useful Representations in a Deep Network with a Local Denoising Criterion,” *J. Mach. Learn. Res.*, vol. 11, pp. 3371–3408, 2010.
21. C. Lu, Z. Y. Wang, W. L. Qin, and J. Ma, “Fault diagnosis of rotary machinery components using a stacked denoising autoencoder-based health state identification,” *Signal Process.*, vol. 130, pp. 377–388, 2017.
22. M. Xia, T. Li, L. Liu, L. Xu, C. W. D. Silva, “Intelligent fault diagnosis approach with unsupervised feature learning by stacked denoising autoencoder,” *Iet. Sci. Meas. Technol.*, vol. 11, no. 6, pp. 687-695, 2017.
23. R. Thirukovalluru, S. Dixit, R. K. Sevakula, N. K. Verma, and A. Salour, “Generating feature sets for fault diagnosis using denoising stacked auto-encoder,” In Proceedings of the IEEE International Conference on Prognostics and Health Management, Chengdu, China ,19-21 October 2016; 1-7.
24. G. Jiang, H. He, P. Xie, and Y. Tang, “Stacked multilevel-denoising autoencoders: a new representation learning approach for wind turbine gearbox fault diagnosis,” *IEEE Trans. Instrum. Meas.*, vol. 99, pp. 1-12, 2017.